

Progressive Failure Analysis of Laminated Composite Beams

YOUNGCHAN KIM,* JULIO F. DAVALOS* AND EVER J. BARBERO**

*West Virginia University
Morgantown, WV 26506-6101*

(Received June 6, 1994)
(Revised February 17, 1995)

ABSTRACT: A progressive failure model for laminated composite beams is formulated using a beam finite element with layer-wise constant shear (BLCS), which permits accurate computation of stresses on each layer. This is the first study to incorporate the stress-prediction accuracy of a layer-wise element for failure prediction of laminates under bending loads. In the present formulation, based on material degradation factors and existing failure criteria, a linear elastic behavior is assumed, and a damaged layer in an element is substituted by a degraded homogeneous layer. Maximum Stress and Tsai-Wu failure criteria are used to assess failure at the Gauss points. The effect of damage accumulation is accounted for by degrading the stiffness properties of failed element-layers in the equilibrium iterations. After equilibrium is satisfied, the load is increased by a constant percentage of first-ply-failure load in a load-controlled failure prediction. A displacement-controlled scheme is also implemented. The predictions of the model correlate well with experimental results for two distinct laminated composite beams: graphite-epoxy and glulam reinforced with GFRP. The study provides guidelines, through parametric studies, for the appropriate selection of material-degradation factors, load increments, and finite element mesh.

KEY WORDS: progressive failure analysis, laminated beam, layer-wise formulation, damage accumulation, stiffness degradation, load-displacement path.

1. INTRODUCTION

NUMEROUS THEORIES FOR the analysis of laminated composite plates and beams have been developed and evaluated. To design efficient composite structures, accurate computation of stresses and reliable predictions of ultimate strengths are necessary. The conventional strength analysis, called total-ply-discount [1], underestimates laminate strength, because it does not recognize that

*Department of Civil and Environmental Engineering and Constructed Facilities Center (CFC).

**Department of Mechanical and Aerospace Engineering and CFC. Author to whom correspondence should be addressed.

ply-failure is localized, and that the remaining stiffness of a failed ply is not necessarily zero. First-ply-failure (FPF) can be predicted easily as long as stresses in a ply are computed accurately. Due to the complexity of composite laminate behavior, a certain degree of discrepancy is expected between failure prediction and actual response of laminates. Also, material inhomogeneity, caused by micro-failures and defects in a laminate, brings additional difficulty in failure modeling, which usually assumes some ideal conditions, such as perfect bonding. Current research is focused on increasing the accuracy for predicting the post FPF behavior of composite laminates. In the post FPF analysis, there are two macroscopic approaches to include damage: modifying the reduced stiffness matrix [2,3,5,6] and degrading the material properties [7-9]. In the former, stiffnesses of failed elements may not be included, whereas, in the latter, degradation level or degradation factor cannot be determined without testing laminates of a material system.

Using the stiffness modification approach, Lee [2] analyzed damage accumulation in composite laminates containing circular holes and subjected to in-plane biaxial loading. He used a failure criterion of his own to define three types of failure mode (fiber breakage, matrix failure, and delamination), in which failure was assessed by using only normal stresses or only shear stresses computed with an 8-node brick element; the representative stresses of an element were computed at the center of the element for fiber and matrix failure, and at the center of an interface for delamination. Upon satisfying equilibrium, or when no further failures were detected in a load step, load was increased to cause the next element to fail. Due to mesh coarseness at the edge of the hole, Lee's program failed to detect delamination and further mesh refinement was impossible because of computational limitations. Ochoa and Engblom [3] used a higher-order plate element and computed transverse stresses from equilibrium equations. The failure analysis procedure was similar to that used by Lee [2], but the stresses for failure prediction were computed at the Gauss points; the reduced stiffness coefficients were modified differently for fiber-breakage failure mode, and a constant load increment was used. Leichti and Tang [4] tried to predict the ultimate load capacity of wood composite I-beams using Tsai-Wu failure criterion and an eight-node plane stress element in ADINA. Because they used a commercial program, the stiffnesses of partially or totally failed elements could not be reduced at the next load step, and the analysis was unable to include cumulative damage effects. Hwang and Sun [5] developed an iterative 3-D finite element analysis with modified Newton-Raphson scheme for the failure prediction of laminates. Tolson and Zabarar [6] followed a similar procedure to that used by Ochoa and Engblom [3], using a higher-order plate element.

Using the material-degradation approach, Tan [7] investigated the progressive failure of laminates with cut-out holes under in-plane tensile loading. A symmetric laminate assumption was used to neglect bending-extension coupling effects, and damage in a lamina was accounted for by using ply-degradation factors. Different degradation factors were used for longitudinal modulus, due to fiber breakage, and for transverse and shear moduli, due to matrix failure. The degradation factors of a material system were adjusted through a parametric study and were

assumed to be independent of lamination sequence. The same approach was extended to a compressive-loading case by Tan and Perez [8]. Reddy and Reddy [9] studied the failure of laminates under axial extension with a finite element implementation of a layer-wise plate theory. They applied a prescribed displacement, for which the load was found by integrating stresses through the thickness. Two different types of stiffness reduction methods were tried: degradation of elastic modulus and Poisson's ratios only; and simultaneous degradation of elastic, shear moduli, and Poisson's ratios. However, material properties were degraded by the same factor regardless of failure modes. They concluded that further investigation was required to apply their approach to laminates under compressive or bending load. Using CLT and total-ply-discount failure analysis, Greif and Chapon [10] conducted three-point bending tests of laminated composite beams and attempted to predict successive failures. After a ply-failure, the analysis was repeated for a new laminate, in which the stiffness of a failed ply was set to zero; this analysis was continued up to five ply-failures. However, their analytical predictions did not match the experimental results.

In previous research [1-3,5-9], mathematical models of varying complexity have been used to investigate failures of laminated composite plates subjected primarily to in-plane loadings. At present, only a few studies have attempted to predict failures of laminated beams under bending [4,10], without providing adequate results.

In the present study, the stress-prediction accuracy of a *Beam* finite element with *Layer-wise Constant Shear* (BLCS) is used to formulate a model for progressive failure of laminated composite beams in bending. The BLCS element can accurately compute normal and shear stresses on each layer. We discuss the finite element implementation of a material-degradation approach for the accurate prediction of failure in laminated composite beams, and we provide guidelines, through parametric studies, for the appropriate selection of degradation factors, load increments, and finite element mesh. Both load- and displacement-controlled schemes are used to trace load-displacement paths to failure. The accuracy of the finite element model is verified with experimental results for two distinct laminates: graphite-epoxy beams [10] and glued-laminated timber beams (glulam) reinforced with pultruded glass-fiber-reinforced plastic (GFRP) [11]. A brief description of the BLCS formulation and failure criteria are presented as a basic background for a detailed description of a progressive failure analysis, illustrated by numerical examples.

2. LAYER-WISE CONSTANT SHEAR BEAM THEORY

The fundamental concepts of layer-wise constant shear beam theory are described briefly, and the details of the finite element formulation can be found in References [12] and [13]. The kinematic assumptions used in BLCS are transverse incompressibility and linear variation of in-plane displacements through the thickness on each layer. Then, the displacements of a point (x - z plane) in a laminated beam are expressed as

where, u
of a point
plane dis
 $\phi^j(z)$. Th
assumptio
stress cor

where \bar{Q}_i
in each l
The valid
et al. [14

where

$$E_x = \bar{Q}_{11}$$

$$G_{xz} = \bar{Q}_{44}$$

In the
points is
stress an
curate, p
predictio
ysis in c

Variou
posed. It
predict f

$$u_1(x,z) = u(x) + \sum_{j=1}^n U^j(x)\phi^j(z), \quad u_2(x,z) = w(x) \quad (1)$$

where, u and w are, respectively, the longitudinal and transverse displacements of a point on the reference axis of the laminate, and $U^j(x)$ represent layer-wise in-plane displacements approximated by linear Lagrange interpolation functions $\phi^j(z)$. The transformed stress-strain relation of an orthotropic lamina under the assumption of plane stress in the x - y plane and without the transverse normal stress component can be written as

$$\begin{pmatrix} \sigma_x \\ \sigma_y \\ \sigma_{xy} \\ \sigma_{yz} \\ \sigma_{zx} \end{pmatrix} = \begin{bmatrix} \bar{Q}_{11} & \bar{Q}_{12} & \bar{Q}_{16} & 0 & 0 \\ \bar{Q}_{12} & \bar{Q}_{22} & \bar{Q}_{26} & 0 & 0 \\ \bar{Q}_{16} & \bar{Q}_{26} & \bar{Q}_{66} & 0 & 0 \\ 0 & 0 & 0 & \bar{Q}_{44} & \bar{Q}_{45} \\ 0 & 0 & 0 & \bar{Q}_{45} & \bar{Q}_{55} \end{bmatrix} \begin{pmatrix} \epsilon_x \\ \epsilon_y \\ \gamma_{xy} \\ \gamma_{yz} \\ \gamma_{zx} \end{pmatrix} \quad (2)$$

where \bar{Q}_{ij} = the transformed reduced stiffnesses. To represent the state of stress in each lamina, the following approximations are used: $\sigma_y = \sigma_{yz} = \sigma_{xy} = 0$. The validation and limitation of this approximation are discussed by Lopez-Anido et al. [14]. Imposing these conditions in Equation (2), we obtain

$$\sigma_x = E_x \epsilon_x, \quad \sigma_{zx} = G_{zx} \gamma_{zx} \quad (3)$$

where

$$E_x = \bar{Q}_{11} + \bar{Q}_{12} \frac{\bar{Q}_{16} \bar{Q}_{26} - \bar{Q}_{12} \bar{Q}_{66}}{\bar{Q}_{22} \bar{Q}_{66} - \bar{Q}_{26} \bar{Q}_{26}} + \bar{Q}_{16} \frac{\bar{Q}_{12} \bar{Q}_{26} - \bar{Q}_{16} \bar{Q}_{22}}{\bar{Q}_{22} \bar{Q}_{66} - \bar{Q}_{26} \bar{Q}_{26}}$$

$$G_{zx} = \frac{\bar{Q}_{45}^2}{\bar{Q}_{44}} + \bar{Q}_{55}$$

In the finite element formulation, a 3-node element with two Gauss integration points is used. Compared with various experimental and analytical examples, the stress and displacement predictions of the BLCS element are remarkably accurate, particularly for soft-core laminated beams [12]. In this study, the stress-prediction accuracy of BLCS is exploited to formulate a progressive failure analysis in conjunction with existing failure criteria.

3. FAILURE CRITERIA

Various failure criteria for isotropic or composite materials have been proposed. It is generally acknowledged that one failure criterion cannot satisfactorily predict failures for all types of laminates. In general, the failure criteria are cate-

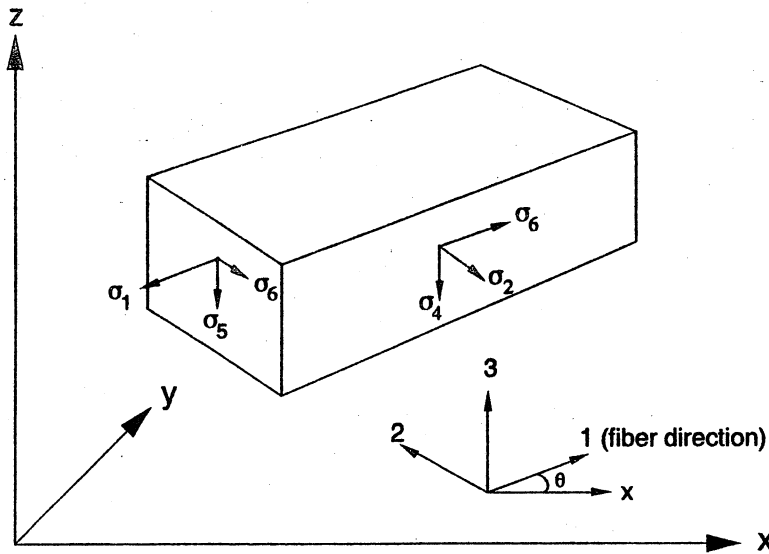


Figure 1. Stress components in the material coordinates.

gorized into two: independent and interactive (or quadratic polynomial) criterion. An independent criterion, such as Maximum Stress or Maximum Strain, is simple to apply and, more significantly, tells the mode of failure, but it neglects the effect of stress interactions in the failure mechanism. An interactive criterion, such as Tsai-Wu, Hoffman, or Hill, includes stress interactions in the failure mechanism, but it does not tell the mode of failure, and it requires some efforts to determine parameters such as F_{12} in the Tsai-Wu criterion. In the present study, two criteria are used: Maximum Stress and Tsai-Wu. All stress components described in Sections 3.1 and 3.2 are with reference to material coordinates, using the contracted notation as shown in Figure 1.

3.1 Maximum Stress Criterion

Failure in a material is assumed if its stress components satisfy one of the following conditions:

$$\begin{aligned}
 \sigma_1 > X_T \quad (\sigma_1 > 0), & \quad \sigma_1 > X_C \quad (\sigma_1 < 0) \\
 \sigma_2 > Y_T \quad (\sigma_2 > 0), & \quad \sigma_2 > Y_C \quad (\sigma_2 < 0) \\
 \sigma_5 > S_{13}, & \quad \sigma_4 > S_{23}
 \end{aligned} \tag{4}$$

where X_T and X_C are, respectively, the tensile and compressive strengths in the longitudinal direction; similarly, Y_T and Y_C are the strengths in the transverse direction, and S_{13} and S_{23} are the shear strengths in 1-3 and 2-3 planes. The mode of failure in a lamina is determined by the specific condition satisfied in Equation (4); for example, if $\sigma_1 > X_T$, it is assumed that the lamina failed due to tensile fiber breakage.

3.2 Tsai-Wu

The criterion is expressed as

where the strength criterion is

$$F_1 \sigma_1$$

where

$$F_1 =$$

$$F_{12} =$$

Since the criterion is determined by the maximum value of the function (6) in terms of the stress components, the failure mode is either fiber or matrix related. The longitudinal strength F_1 and the transverse strength F_2 are related to the Tsai-Wu criterion by the following equations:

The failure mode is determined by the maximum value of the damage function. The failure mode is either fiber or matrix related. The longitudinal strength F_1 and the transverse strength F_2 are related to the Tsai-Wu criterion by the following equations:

3.2 Tsai-Wu Criterion

The most general quadratic polynomial criterion is given by Tsai-Wu and written as

$$f(\sigma) = F_i \sigma_i + F_{ij} \sigma_i \sigma_j \quad i, j = 1, 2, \dots, 6 \quad (5)$$

where σ_i are stress tensor components in material coordinates, and F_i and F_{ij} are strength tensors. For a transversely isotropic lamina in the 2-3 plane, the criterion is expanded as follows:

$$F_1 \sigma_1 + F_2 \sigma_2 + F_{11} \sigma_1^2 + F_{22} \sigma_2^2 + 2F_{12} \sigma_1 \sigma_2 + F_{44} \sigma_4^2 + F_{66} (\sigma_5^2 + \sigma_6^2) = 1 \quad (6)$$

where

$$F_1 = \frac{1}{X_T} - \frac{1}{X_C}, \quad F_2 = \frac{1}{Y_T} - \frac{1}{Y_C}, \quad F_{11} = \frac{1}{X_T X_C}, \quad F_{22} = \frac{1}{Y_T Y_C}$$

$$F_{12} = -\frac{1}{2\sqrt{F_{11} F_{22}}}, \quad F_{44} = \frac{1}{S_{23}^2}, \quad F_{66} = \frac{1}{S_{13}^2}$$

Since the Tsai-Wu criterion does not describe failure modes, these are determined by the strength tensors associated with normal stresses or shear stresses, whichever provide the most contribution to a failure. The first five terms of Equation (6) are related to normal stress failure and denoted as C_N , and the last two terms are associated with shear stress failure and denoted by C_S . Then, in a failure analysis, if $C_N > C_S$, it is assumed that the failure is due to normal stresses either in the longitudinal (fiber failure related to σ_1) or transverse (matrix failure related to σ_2) direction. To further decide whether the failure is dominated by the longitudinal or transverse normal stress, the sum of the terms corresponding to F_1 and F_{11} , referred to as C_N^L , is compared to the sum of the terms related to F_2 and F_{22} , referred to as C_N^T . If $C_N^T > C_N^L$, it is assumed that failure occurs in the transverse direction; a matrix-dominated failure. Both Maximum Stress and Tsai-Wu criteria are used in this study for progressive failure analysis of laminated beams.

4. PROGRESSIVE FAILURE ANALYSIS

The progressive failure analysis presented in this paper is based on the assumption that a material is linear elastic up to ultimate failure. The stiffness of a damaged layer over a discrete length is replaced by a homogeneous degraded layer whose material properties are a constant multiple of original properties. Material degradation factors (DFs) are used to define a percentage of the stiffness retained in a ply after micro-damage has occurred. DFs are widely used in macroscopic damage modeling, but unfortunately there are no explicit formula-

tions to predict them, and only a few studies have presented parametric studies to evaluate the effect of DFs in failure analyses [7-9]. A degradation factor is used to globally adjust the local stiffness degradation of a ply over a finite region. Distinct degradation factors are used for fiber failure and matrix failure, and when combined with failure criteria, the normal stress components are associated with fiber breakage and the transverse normal and shear stresses are related to matrix failure. Since a degradation level depends among other factors on crack density and lamination sequence, as observed in an experimental evaluation of cross-ply laminates under uniaxial tension [15], an accurate evaluation of DFs is a difficult task, which complicates the implementation of numerical methods in macroscopic damage modeling. In this paper, we illustrate with examples a procedure for selecting DFs for specific material systems, by conducting parametric studies and correlating the predicted ultimate loads with experimental values. This procedure is applied to two types of laminated beams: graphite-epoxy and laminated wood reinforced with pultruded glass/vinylester strips. Once specific DFs for a material system are selected by establishing acceptable correlations with experimental data, they are used consistently throughout the analyses to trace load-displacement paths to failure. Degradation factors for fiber (DF_f) and matrix (DF_m) are used to define degraded material properties, denoted by a superscript d , in terms of original properties, denoted by a superscript o , as:

- for failure related to normal stress in the fiber direction (i.e., fiber breakage)

$$E_1^d = (DF_f)E_1^o, \quad G_{12}^d = (DF_f)G_{12}^o, \quad \nu_{12}^d = (DF_f)\nu_{12}^o$$

- for failure related to normal stress in the transverse direction (i.e., matrix failure)

$$E_2^d = (DF_m)E_2^o, \quad G_{12}^d = (DF_m)G_{12}^o$$

$$G_{23}^d = (DF_m)G_{23}^o, \quad \nu_{21}^d = (DF_m)\nu_{21}^o$$

- for failure related to shear stresses (a matrix dominated failure)

$$G_{12}^d = (DF_m)G_{12}^o, \quad G_{23}^d = (DF_m)G_{23}^o$$

Consider for example the effect of DFs on the failure prediction of a laminated beam under bending. If most fibers are oriented at 0° , the failure prediction will be more sensitive to the DF for fiber than for matrix; in contrast, if most fibers are oriented at 90° , the DF for matrix will be significant in failure prediction; finally, for crossply and angleply combinations, the relative values of both factors will affect the failure prediction.

In the present study, the progressive failure analysis with a load-controlled scheme proceeds with the following algorithm:

1. Com
- and
2. Find
- stress
- decr
- R_{min}
3. Inpu
4. Deg
- whic
- failu
- load
5. Chec
- wise
6. Repe
- occu

In the loading applied ply-failure FPF dis 3-node b putation pendix. trate the schemes

Since accuracy with a g computa experim epoxy an

5.1 Gra

Greif a made of strength inate typ specifica specimen ment, an trace the

1. Compute stresses for an initial prescribed loading at the reduced Gauss points and check failure with a selected failure criterion.
2. Find the minimum ratio between the ultimate material strength and applied stress; i.e., the strength ratio, R_{min} , for the initial loading. If $R_{min} \leq 1$, then, decrease the initial loading to a small enough value not to cause failure. If $R_{min} > 1$, then, increase the load by R_{min} and find first-ply-failure load.
3. Input a set of degradation factors: DF_f and DF_m .
4. Degrade material properties at Gauss points according to failure modes, which are established by determining the dominant stress components in the failure criteria, as explained before. Then, compute stresses at the current load.
5. Check for subsequent failures. If failures are detected, go to step 4. Otherwise, increase the load by a given constant percentage of FPF load.
6. Repeat steps 4 to 5 until ultimate failure is reached, which is defined as the occurrence of failures through the thickness of a laminate at a given point.

In the displacement-controlled scheme, displacements are prescribed at the loading points, and using the equilibrium of vertical forces, the corresponding applied loads are computed from the reaction forces at the supports. After first-ply-failure, prescribed displacements are increased by a constant percentage of FPF displacement. The progressive failure algorithm is incorporated into a 3-node beam finite element with layer-wise constant shear (BLCS), and the computational procedure to modify the stiffness coefficients is described in the Appendix. The experimental results for two types of laminates are used next to illustrate the selection of load/displacement increments and DFs and computational schemes to trace load-displacement paths to failure with the present formulation.

5. NUMERICAL EXAMPLES

Since a failure assessment is based on the magnitude of stresses at a point, the accuracy of the computed stresses is a determining factor for failure prediction with a given failure criterion. In this study, the capability of BLCS for stress computation and subsequent failure prediction is demonstrated by analyzing the experimental results of laminated composite beams of two types: (1) graphite-epoxy and (2) GFRP-glulam.

5.1 Graphite-Epoxy Beams

Greif and Chapon [10] conducted three-point bending tests of composite beams made of AS4/3502 graphite-epoxy pre-preg tape; the material properties and strength parameters of the test-specimens are listed in Table 1. Five different laminate types were tested, with two specimens for each type, and the test beam specifications are given in Table 2. The progressive failure analysis of the test specimens is based on appropriate selections of finite element mesh, load increment, and degradation factors, and on appropriate implementation of schemes to trace the load-displacement responses to failure.

Table 1. Material properties and strength parameters.

Material Properties	Strength Parameters (GPa)
$E_1 = 141.2$ GPa	$X_T = 2.343$
$E_2 = 11.5$ GPa	$X_C = 1.723$
$G_{12} = 6.0$ GPa	$Y_T = 0.051$
$\nu_{12} = 0.3$	$Y_C = 0.223$
	$S_{12} = 0.009$

Note: in BLCS, $S_{13} = S_{23} = S_{12}$ is used.

Table 2. Beam specifications.

Laminate	Lay-Up	No. of Plies	Length (mm)	Width (mm)	Thickness (mm)
A1	$[90_s/0_s]_s$	32	139.7	24.84	4.648
A2	$[90_s/0_s]_s$	32	152.4	25.65	4.547
B1	$[0_s/90_s]_s$	32	127.0	24.13	4.597
B2	$[0_s/90_s]_s$	32	152.4	24.69	4.674
C1	$[(0/90)_s]_s$	32	152.4	25.65	4.470
C2	$[(0/90)_s]_s$	32	152.4	24.33	4.470
D1	$[(45/0/-45)_s]_s$	30	152.4	24.26	4.166
D2	$[(45/0/-45)_s]_s$	30	152.4	24.46	4.166
E1	$[(0/45/0/-45)_s/90/0/0_{1/2}]_s$	29	152.4	24.49	4.039
E2	$[(0/45/0/-45)_s/90/0/0_{1/2}]_s$	29	152.4	25.30	4.039

5.1.1 FE

In the first simulation, a mesh of 2000 elements was required to obtain convergence. The number of elements used in the subsequent simulations was 10000.

In a test, the displacement increment was 0.1 mm. The load or force was applied to the free end of the beam. A load of 10 kN was applied to the very small area of the first-ply-failure scheme. The FPF load must be determined. It should be determined. In the A2, C2, and E2, the ultimate load increment and ultimate

5.1.1 FE MESH AND LOAD INCREMENT

In the finite element analysis, it is well established that mesh refinement is required until displacements or stresses converge within a desired accuracy. Figure 2 obtained with the Tsai-Wu failure criterion and a load-controlled scheme shows convergence trends of ultimate failure load for typical graphite-epoxy test-samples. A mesh refinement for ultimate failure loads show stable trends at fourteen elements, and hereafter, all analyses are carried out using 14 elements and the number of layers for each laminate as listed in Table 2.

In a test, the load and displacement increase continuously, but in a numerical simulation, discrete load or displacement increments are used in a load- or displacement-controlled failure prediction scheme. Thus, the load or displacement increments, defined in this study as a constant percentage of first-ply-failure load or first-ply-failure displacement, will affect the damage evolution in a laminate. A large load increment may not represent damage progression well, and a very small load increment may require a significant computational effort. After first-ply-failure (FPF) is reached and equilibrium is satisfied in a load-controlled scheme, the load is increased by a constant percentage of FPF load, but since FPF loads of laminates vary considerably, a judicious choice of load increment must be used in the analysis, and the appropriate load percentage to be used should be determined parametrically, as shown in Figure 3 for the Tsai-Wu criterion. In Figure 3, laminate B2 is more sensitive to load increment than laminates A2, C2, D2, and E2, because the FPF load of laminate B2 is within 5% of its ultimate failure load. The FPF and ultimate failure loads can be used to define the load increments to be used in the analysis; when the difference between FPF load and ultimate load is small, the laminate failure mode is usually brittle and sud-

Thickness (mm)
4.648
4.547
4.597
4.674
4.470
4.470
4.166
4.166
4.039
4.039

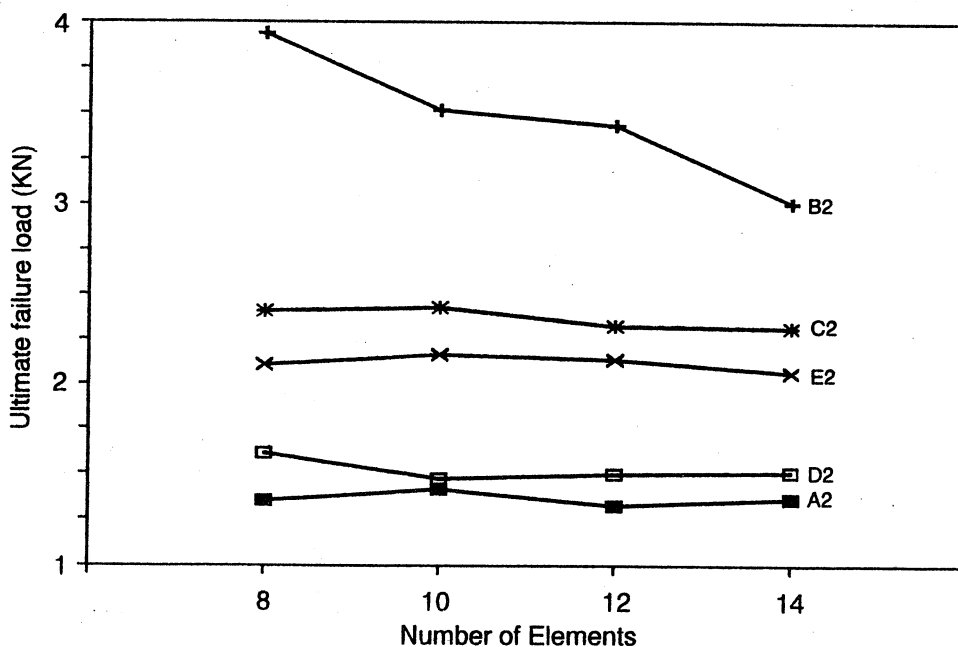


Figure 2. Convergence of ultimate failure load.

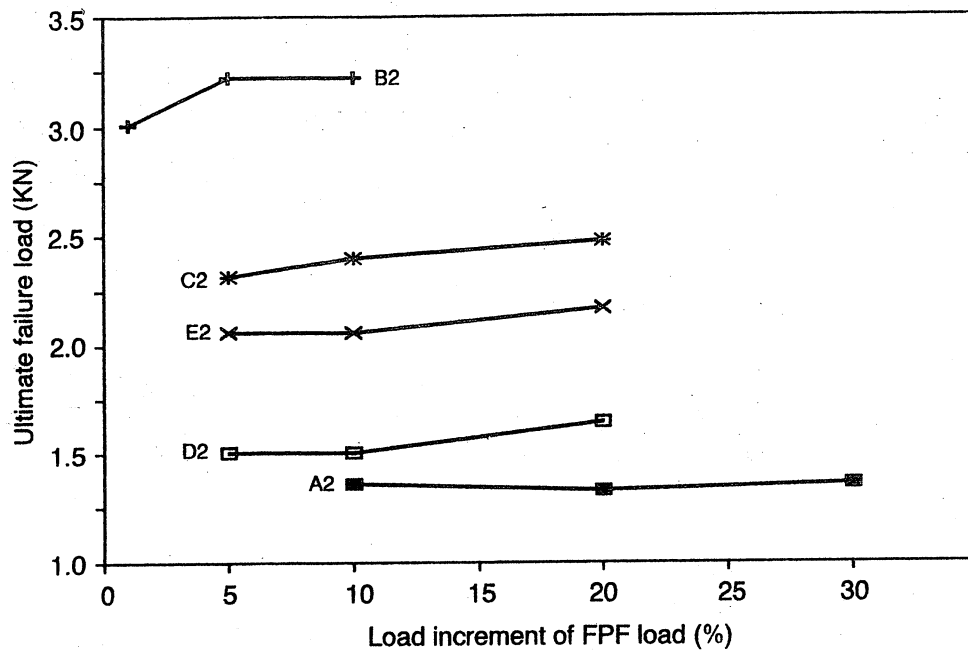


Figure 3. Effect of load increment on ultimate failure load.

den, which is the case for laminates B, and in this case a small load increment should be used. The results shown in Figure 3 are used to select the following load increments: 10% for laminate A, 1% for laminate B, and 5% for laminates C, D, and E for the load-controlled scheme. A similar study is conducted to define the displacement increments as 5% of FPF displacement for all the laminates. The results in Figures 2 and 3 are obtained with $DF_f = 0.25$ and $DF_m = 5 \times 10^{-3}$, which are selected through a parametric study as explained next.

5.1.2 DEGRADATION FACTORS

As damages evolve in laminates, degradation factors play a key role in redistributing stresses and finally determining ultimate strength. In Table 3, the dependency of ultimate strength on degradation factors for fiber (DF_f) and matrix (DF_m) is illustrated using the Tsai-Wu criterion; each set of degradation factors is represented in the form (DF_f, DF_m) . For laminates B and C, an increase of matrix degradation factor results in higher ultimate strengths, because in both laminates failure starts and propagates in the 90° layers. For laminate A, failure initiates in the 90° layers, but the 0° layers provide most of the flexural resistance, and therefore, the laminate strength depends on both degradation factors. The same trend can be observed for the angleply laminates D and E. As mentioned in the introduction, the other macroscopic approach of damage modeling is to modify the reduced stiffness matrix, which is similar to using very small degradation factors. Compared to experimental values, the ultimate loads obtained with the set $(10^{-6}, 10^{-6})$ are mostly underestimated, leading to a maximum error of 24.4% for laminate C1 (Table 3). According to Reddy and Reddy [9], the set $(10^{-1}, 10^{-1})$ provided very good prediction for laminates under uniaxial tension.

increment following laminates ducted to the lami-
 $DF_m =$
 next.

in redis-
 the de-
 and matrix
 n factors
 crease of
 e in both
 A, failure
 ral resis-
 n factors.
 As men-
 modeling
 very small
 oads ob-
 maximum
 y [9], the
 tension.

Table 3. Effect of degradation factors on ultimate failure load (N): load-controlled.

DF _f	DF _m	A1	A2	B1	B2	C1	C2	D1	D2	E1	E2
10 ⁻⁶	10 ⁻⁶	1080	1110	3400	2820	1920	1820	1290	1300	1680	1740
10 ⁻⁶	10 ⁻¹	1110	1140	3740	3360	2090	1980	1320	1340	1730	1790
10 ⁻¹	10 ⁻⁶	1080	1110	3400	2820	1920	1820	1290	1300	1730	1790
10 ⁻¹	10 ⁻¹	1570	1330	3740	3360	2230	2110	1360	1370	1840	1900
0.25	5 x 10 ⁻³	1290	1360	3400	3010	2440	2310	1490	1500	1990	2060
Experiment [10]		1310	1250	2800	2850	2540	2400	1600	1560	2050	2000

However, as seen in Table 3, the present predictions with the set $(10^{-1}, 10^{-1})$ are not satisfactory. The discrepancy with the results of Reference [9] is probably due to differences in materials and loading conditions. The set $(0.25, 0.005)$ gives very good predictions with a maximum error of 21.4% for laminate B1 (Table 4). This maximum error may be due to the unreliable experimental value reported for laminate B1; since laminate B1 is 20% shorter than B2 (Table 1), the ultimate load for laminate B1 should be approximately 20% higher than that of laminate B2, or about 3420 N as predicted by the analysis.

In the study of laminates containing holes under in-plane tension [7] and compression [8], good predictions were obtained with the sets $(0.07, 0.2)$ for tensile loading and $(0.14, 0.4)$ for compressive loading. Even though direct comparison of those results with the present study is not adequate, because of differences in materials and loading, the use of different factors for fiber and matrix seems to provide better results in macroscopic damage modeling. In Table 5, FPF load predictions with BLCS are compared with those of Reference [10], in which CLT coupled with total-ply-discount (TPD) is used. FPF predictions by Tsai-Wu and Maximum Stress criteria with BLCS are consistently close to each other, on the other hand, the prediction by Maximum Stress criterion with TPD is very high for laminate D2. Similarly, the comparisons of ultimate failure loads with the results of Reference [10] (TPD) are given in Table 4. The TPD predictions were obtained through 5 successive failures, and as expected, these predictions are unreliable and usually too conservative. The predictions with BLCS and Maximum Stress criterion are consistently higher than those with Tsai-Wu criterion; this is probably due to the increased contribution of shear stresses to failure in the Tsai-Wu criterion at higher load levels. These differences, however, are not significant for the FPF predictions (see Table 5). A discussion of the prediction of the load-displacement path to failure is presented next.

Table 4. Ultimate failure load (N): load-controlled.

Laminate	Experiment [10]	Tsai-Wu Criterion		Maximum Stress Criterion	
		Ref. [10]	BLCS	Ref. [10]	BLCS
A1	1310	380	1290	380	1480
A2	1250	—	1360	—	1460
B1	2800	5310	3400	4230	4490
B2	2850	—	3010	—	3880
C1	2540	1940	2440	1970	2490
C2	2400	—	2310	—	2360
D1	1600	—	1490	—	1530
D2	1560	850	1500	1150	1540
E1	2050	—	1990	—	2270
E2	2000	—	2060	—	2350

Lamina

A1
A2
B1
B2
C1
C2
D1
D2
E1
E2

5.1.3 L

As the
placem
ultimat
num di
mate lo
enginee
Table 6
displac
a load i

Table 5. FPF load (N): load-controlled.

Laminate	Tsai-Wu Criterion		Maximum Stress Criterion	
	Ref. [10]	BLCS	Ref. [10]	BLCS
A1	329	307	334	307
A2	—	316	—	316
B1	3248	3039	3315	3115
B2	—	2688	—	2732
C1	921	872	925	872
C2	—	828	—	828
D1	—	676	—	672
D2	845	685	1005	672
E1	—	1050	—	1032
E2	—	1090	—	1068

5.1.3 LOAD-DISPLACEMENT PATH

As the progressive failure analysis algorithm approaches ultimate load, the displacement can become significantly large for a small increase in load, until the ultimate load is reached, and therefore, it may be difficult to predict the maximum displacement at ultimate load. However, the displacement plateau near ultimate load can be used to terminate the analysis and predict ultimate load within engineering accuracy. Based on this observation, the displacements listed in Table 6 are those corresponding to ultimate load or near-ultimate-load. These displacements were used to check the admissibility of a final load increase, where a load increment causing a displacement far beyond the experimental displacement.

Table 6. Ultimate displacement (mm): load-controlled.

Laminate	Experiment [10]	BLCS	
		TW ^a	MS ^b
A1	20.1	17.8	27.2
A2	30.5	21.6	27.7
B1	6.4	6.1	9.9
B2	10.4	9.3	17.4
C1	15.2	18.9	15.0
C2	15.0	18.9	15.0
D1	16.0	15.6	17.3
D2	15.8	15.6	17.3
E1	15.8	18.1	19.1
E2	15.0	18.1	19.1

^aTW = Tsai-Wu criterion.

^bMS = Maximum Stress criterion.

ment at ultimate load was considered artificial and physically unacceptable. The predicted and experimental ultimate loads and displacements are compared graphically in Figures 4 and 5, respectively, where the predicted values by the present analysis and Reference [10] are obtained with the Tsai-Wu criterion. The data points below the 45° diagonal line underpredict the response and those above overpredict the response. For the ultimate load comparisons (Figure 4), the BLCS data points are clustered around the diagonal line, but the analytical values of Greif and Chapon [10] are farther away from the diagonal line. The data points for ultimate displacement show a larger scatter than those for ultimate load (Figure 5), particularly for laminate A2, which exhibited significant nonlinearity in the experimental testing. In general, the load- and displacement-controlled schemes predicted similar results.

The predicted load-displacement diagrams for all the graphite-epoxy laminates are given in Reference [16], and typical curves for laminates A1, B2, and D2 are shown in Figures 6, 7, and 8. In these figures, the displacement plateau at ultimate load of the load-controlled scheme has been omitted, and the predicted ultimate failure points for both schemes are specifically shown. These figures illustrate typical prediction curves for crossply (Figures 6 and 7) and angleply (Figure 8) laminates in comparison with experimental curves; the prediction curves show slope changes that result from damage detection and progression in the BLCS analysis. In general, BLCS predicts stiffer responses, but the slopes of the BLCS prediction curves near ultimate failure are close to those of the experimental curves, which indicate that the damage progression in BLCS is properly repre-

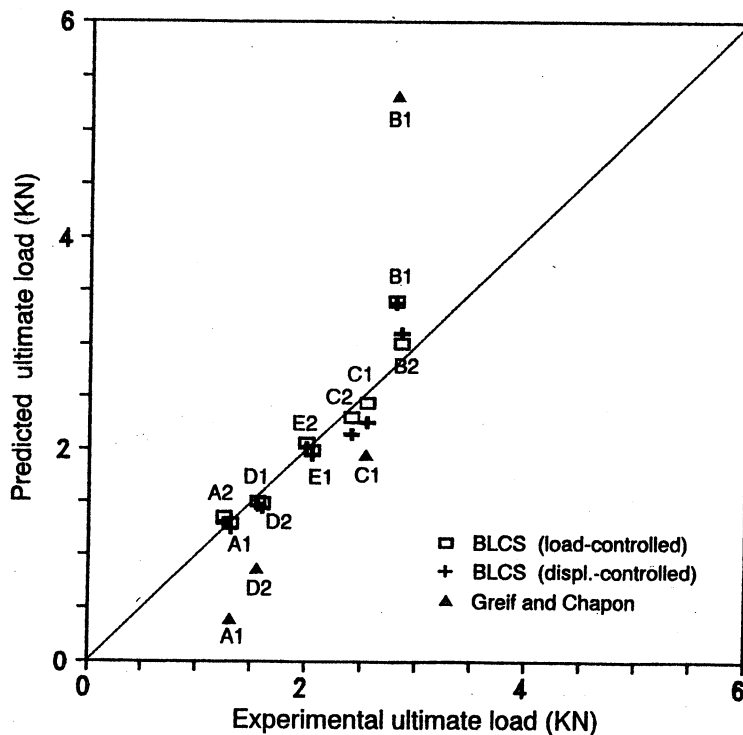


Figure 4. Comparison of ultimate failure load.

ptable. The compared lues by the terion. The and those gure 4), the tical values data points imate load onlinearity -controlled

laminates und D2 are at ultimate d ultimate s illustrate (Figure 8) rves show the BLCS the BLCS perimental rly repre-

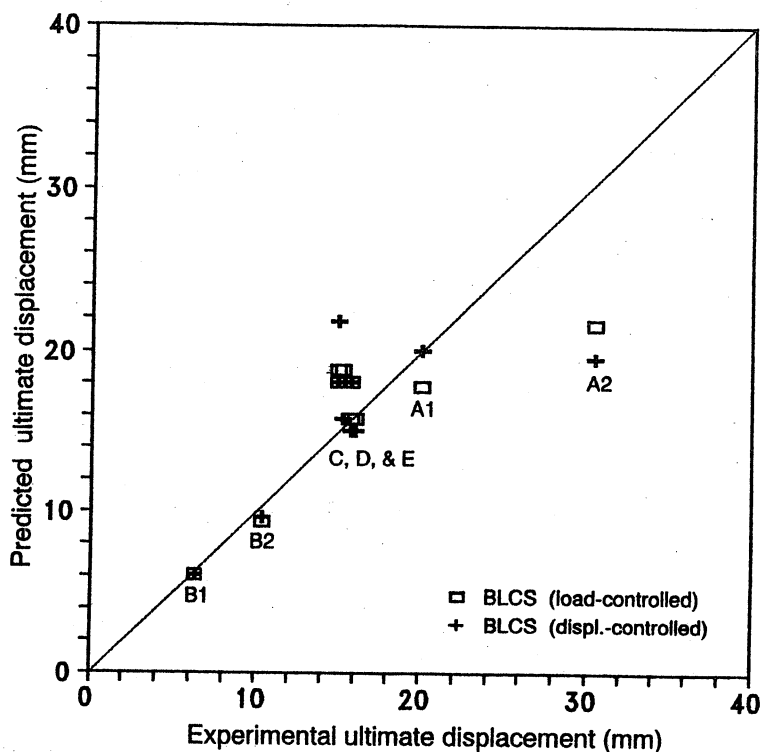


Figure 5. Comparison of ultimate displacement.

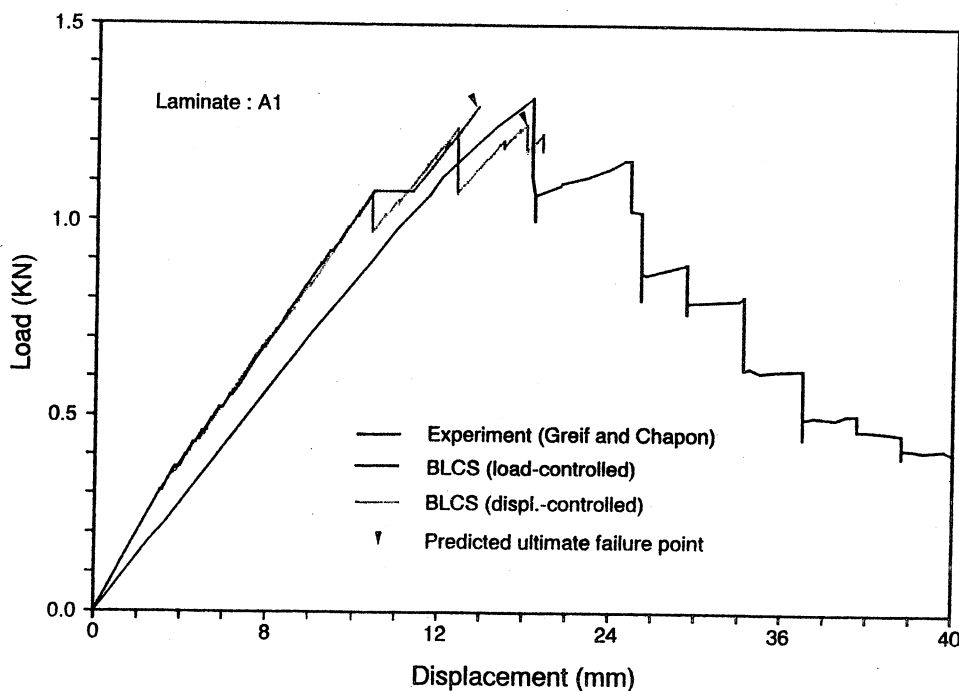


Figure 6. Load-displacement path: laminate A1.

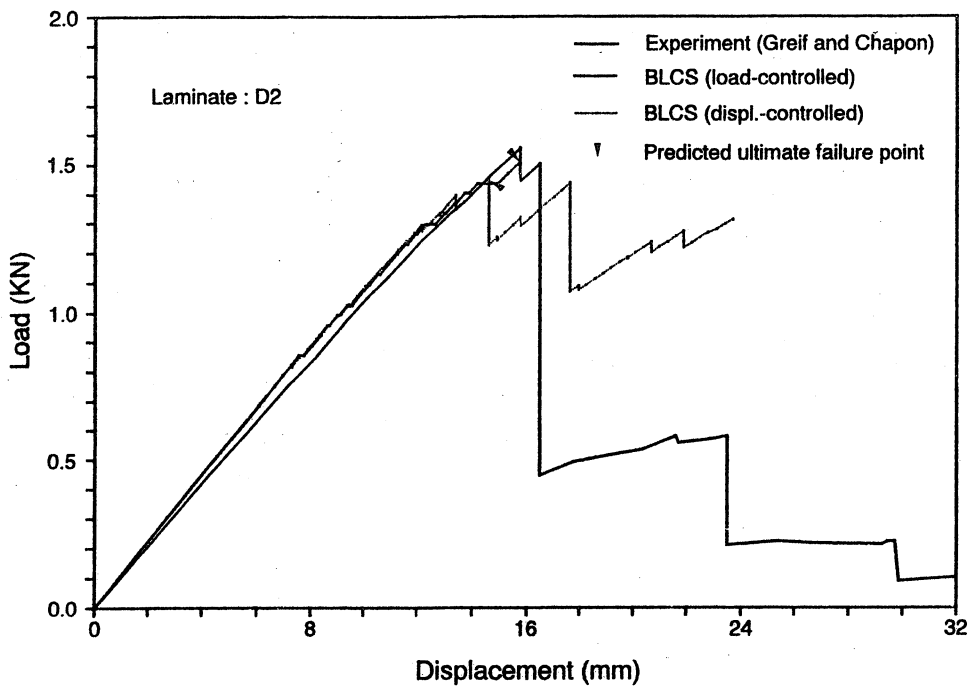


Figure 7. Load-displacement path: laminate D2.

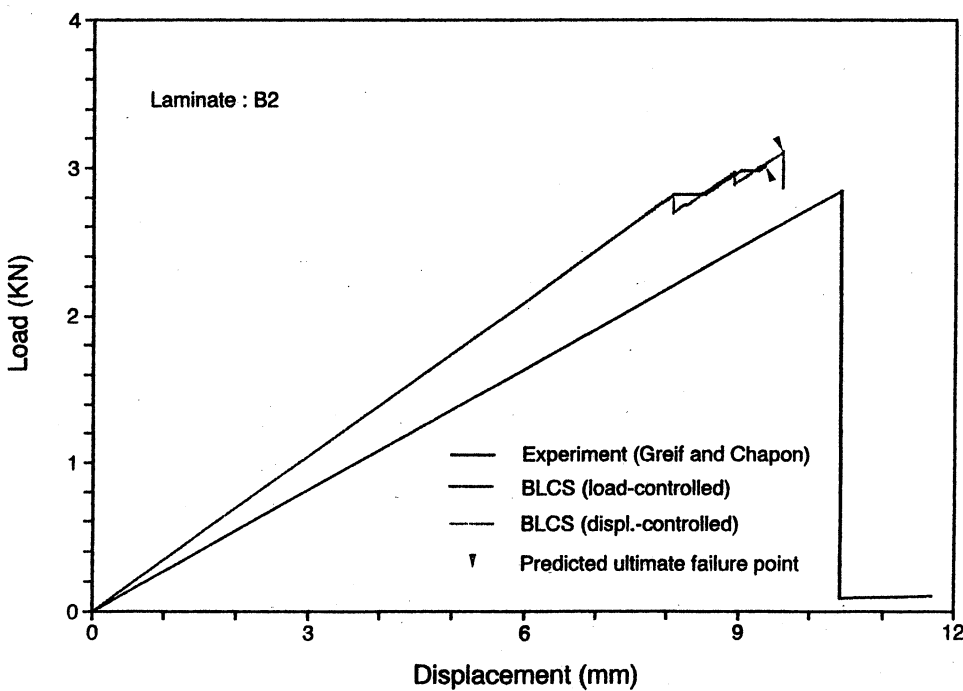


Figure 8. Load-displacement path: laminate B2.

Progress

sented.
 ing of t
 before t
 matrix
 samples
 factors
 dictions
 the Ma
 perimen

5.2 Glu

Gluec
 arches,
 and stre
 resulting
 buckling
 member
 [11] con
 beams r
 six woo
 nesses a
 layer. A
 rameter
 $X_T = 5$
 cussed i
 beams,
 load inc
 values. I
 strip ren
 placeme
 with the
 sponse,
 loads we
 the ultir
 The pr
 controll
 differen
 2 is sho
 to comp
 displac
 increas
 Therefo
 the disp
 tion cur
 laminate

sented. The discrepancy with the experimental behavior is due in part to the aging of the test-specimens, which were fabricated at NASA two or more years before they were tested. As the authors stated, the deterioration of the epoxy matrix probably resulted in stiffness reduction of the laminates, particularly for samples A and B which exhibited a response-sensitivity to matrix degradation factors (Table 3). Considering both ultimate failure load and displacement predictions for this example, the Tsai-Wu failure criterion predicts better results than the Maximum Stress criterion. The present model correlates well with the experimental results.

5.2 Glulam-GFRP Beams

Glued-laminated timber beams (glulam) are used for large-span bridges, arches, frames, and reticulated domes. Due to the relatively low bending stiffness and strength of glulam, long-span structures require members of larger depths, resulting in member-weight increase and bracing requirement to prevent lateral buckling. One way to increase stiffness and strength of glulam is to reinforce members with glass fiber-reinforced plastic (GFRP) composites. Davalos et al. [11] conducted four-point bending tests of 122-cm long and 5.6-cm wide glulam beams reinforced with GFRP strips at the bottom. The beams were composed of six wood layers and one GFRP bottom layer, with material properties and thicknesses as given in Table 7, where layer number one corresponds to the top wood layer. As the laminates are unidirectionally reinforced, the required strength parameters given in MPA are: for GFRP, $X_T = 248.2$ and $S_{13} = 70.3$; for wood, $X_T = 54.8$, $X_C = 58.6$, and $S_{13} = 12.4$. Parametric studies similar to those discussed in the previous section were undertaken. Throughout the analysis of the beams, a fourteen-layered 30 element mesh was used in conjunction with a 1% load increment or a 10% displacement increment of the corresponding FPF values. In the experiment and also in the BLCS prediction, the GFRP reinforcing strip remained intact at ultimate load. In Table 8, the prediction of loads and displacements are compared with experimental results. The predictions are obtained with the set $(10^{-1}, 10^{-1})$. To find out the effect of degradation factors on the response, the set $(10^{-6}, 10^{-6})$ is also used, and interestingly, the predicted ultimate loads were identical to the FPF loads listed in Table 8 for the set $(10^{-1}, 10^{-1})$. Thus, the ultimate loads with $(10^{-6}, 10^{-6})$ were underpredicted by approximately 25%. The predictions with the Maximum Stress criterion in the displacement-controlled formulation match closely the experimental results, with a maximum difference of 6% for beam 3. The experimental load-displacement curve for beam 2 is shown in Figure 9, and it exhibits a nonlinear behavior near 35 KN due to compression failure of the upper wood lamina. The prediction of load-displacement paths with the displacement-controlled scheme showed a small load increase after a large displacement increase, which is physically inadmissible. Therefore, the ultimate failure point is assumed to correspond to the beginning of the displacement plateau. Since linear behavior is assumed in BLCS, the prediction curve for this beam cannot trace precisely the experimental path. For these laminates, the predictions with Maximum Stress criterion are relatively close to

Table 7. Material properties for GFRP-glulam.

Layer No.	E_1 (GPa)			G_{13} (GPa)			Thickness (mm)		
	Beam 1	Beam 2	Beam 3	Beam 1	Beam 2	Beam 3	Beam 1	Beam 2	Beam 3
1	17.66	14.93	15.63	1.021	0.620	0.668	19.33	19.38	19.41
2	14.02	13.39	13.21	0.634	0.641	0.700	19.43	19.43	19.43
3	14.33	14.83	13.82	0.628	0.653	0.641	19.46	19.33	19.46
4	11.88	13.02	12.44	0.915	0.647	0.796	19.33	19.35	19.48
5	17.96	14.20	14.10	0.871	0.588	0.666	19.33	19.35	19.43
6	14.83	16.71	17.13	0.621	1.048	0.630	19.43	19.48	19.43
7	19.69	19.69	19.69	3.803	3.803	3.803	9.398	9.398	9.398

Beam
No.

1

2

3

Table 8. Comparison of loads and displacement for glulam-GFRP (units: KN, mm).

Beam No.	Loads and Displacement	Load-Controlled		Displacement-Controlled		Experiment
		TW	MS	TW	MS	
1	FPF Load	32.69	32.83	32.65	32.83	—
	Failure Load	42.48	45.68	45.19	44.48	44.48
	Displacement	10.74	12.60	11.38	11.43	18.16
2	FPF Load	37.05	37.14	37.05	37.14	—
	Failure Load	45.19	42.35	46.17	46.84	48.93
	Displacement	12.62	10.72	12.78	12.83	17.78
3	FPF Load	35.85	35.94	35.90	36.00	—
	Failure Load	44.79	44.93	45.91	46.08	48.93
	Displacement	11.96	11.91	12.01	12.07	11.73

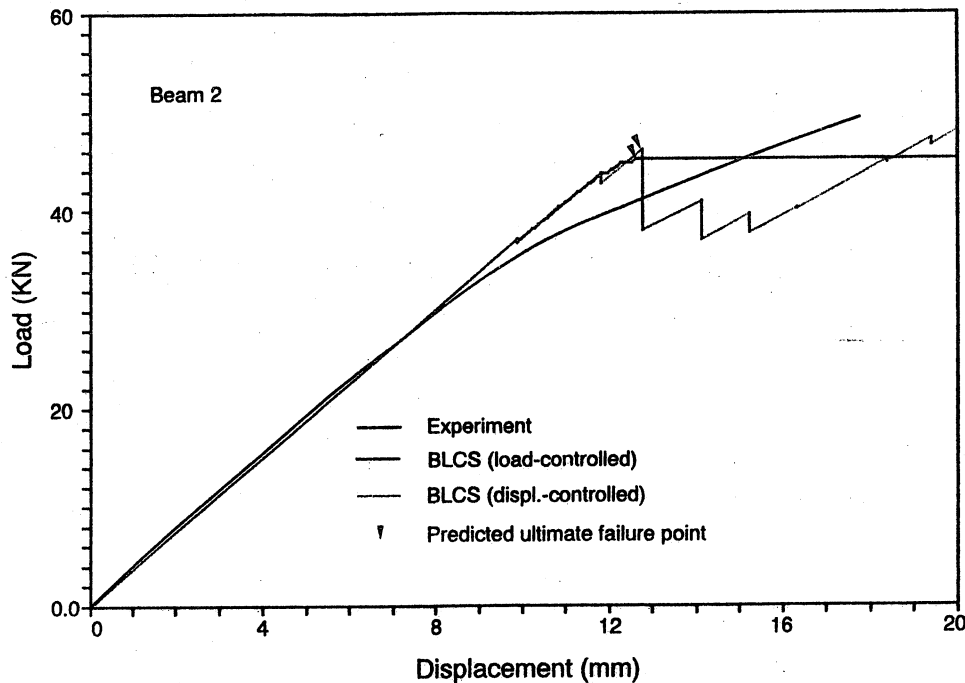


Figure 9. Load-displacement path: glulam-GFRP beam 2.

those with Tsai-Wu criterion. Once again, the present formulation with BLCS accurately predicts the ultimate failure load of the glulam-GFRP samples.

6. CONCLUSION

The present progressive failure model for laminated composite beams under bending is the first study that successfully integrates the stress-accuracy of a layer-wise formulation with a material-degradation scheme to accurately predict bending failures. A 3-node beam element with layer-wise constant shear (BLCS) is used, and the element stresses at each layer are computed at the Gauss points. Different degradation factors for fiber and matrix are used, and these are defined through parametric studies and experimental results for specific material systems. The following specific conclusions are presented:

1. The present formulation, based on material-degradation and existing failure criteria, can accurately predict the progressive failure and ultimate load of laminated composite beams, as verified by experimental results of graphite-epoxy and GFRP-glulam samples.
2. The main advantage of the layer-wise formulation is the possibility of modifying material properties either at top or bottom of each element-layer, since degrees of freedom are defined at these locations. This results in a much more efficient modeling of failure-degradation than in single-layer formulations.
3. Degradation factors, load increments, and mesh refinement should be established for a specific material system through parametric studies and using experimental data.

Progressive

4. When
or ne
deflec

5. The
glula
(a)

(b)

(c)

(d)

6. The
pred
nonl

Compu

To ill
expressi
neous e

The s

4. When a load-controlled formulation is used, the large displacement-plateau at or near ultimate load can be used to terminate the analysis, since such a large deflection under constant load is physically inadmissible.
5. The present failure analysis with BLCS of the graphite-epoxy [10] and glulam-GFRP [11] samples indicate the following:
 - (a) The Tsai-Wu criterion provides more reliable results than the Maximum Stress criterion, but for the glulam-GFRP beams, both criteria combined with the displacement-controlled scheme produced consistent results.
 - (b) In general, distinct degradation factors for fiber and matrix should be used.
 - (c) While the ultimate loads can be predicted with sufficient accuracy, the ultimate maximum displacements can vary as much as 30% from the experimental results.
 - (d) Finally, the experimental data considered in this study is not sufficient to make more general conclusions, and more extensive correlations are desirable.
6. The present study offers great potential for further improvement of failure-prediction of laminated beams under combined loading, by considering nonlinear material and/or geometric effects.

APPENDIX

Computation of Stiffness Coefficients

To illustrate the scheme for incorporating a damage formulation in BLCS the expressions for the stiffness coefficients are presented. In BLCS, the N simultaneous equations for the element model are written as follows:

$$\begin{bmatrix} [A_1] & [B_1] & [B_2] & \dots & [B_N] \\ [B_1]^T & [D_{11}] & [D_{12}] & \dots & [D_{1N}] \\ \cdot & \cdot & \cdot & \dots & \cdot \\ [B_N]^T & [D_{N1}] & [D_{N2}] & \dots & [D_{NN}] \end{bmatrix} \begin{Bmatrix} \{\Delta^0\} \\ \{\Delta^1\} \\ \cdot \\ \{\Delta^N\} \end{Bmatrix} = \frac{1}{b} \begin{Bmatrix} \{F\} \\ \{F_x^1\} \\ \cdot \\ \{F_x^N\} \end{Bmatrix}$$

The submatrices are

$$[A_i] = \int_0^L [B_L]^T [A][B_L] dx$$

$$[B_i] = \int_0^L [B_L]^T [B^i][\bar{B}_L] dx$$

$$[D_{ij}] = \int_0^L [\bar{B}_L]^T [D^{ij}][\bar{B}_L] dx$$

where

$$[A] = \begin{bmatrix} a_1 & 0 \\ 0 & a_2 \end{bmatrix}, \quad [B^i] = \begin{bmatrix} b_1^i & 0 \\ 0 & b_2^i \end{bmatrix}, \quad [D^{ij}] = \begin{bmatrix} d_1^{ij} & 0 \\ 0 & d_2^{ij} \end{bmatrix}$$

B_L and \bar{B}_L are compatibility matrices. The stiffness coefficients are computed as

$$a_1 = \sum_{k=1}^N E_x^k h^k, \quad a_2 = \sum_{k=1}^N G_{xz}^k h^k$$

where h is the thickness of a layer.

For $i = j$:

$$b_1^1 = E_x^1 \frac{h^1}{2}, \quad b_2^1 = -G_{xz}^1 \quad (j = 1)$$

$$b_1^j = E_x^{j-1} \frac{h^{j-1}}{2} + E_x^j \frac{h^j}{2}, \quad b_2^j = G_{xz}^{j-1} - G_{xz}^j \quad (2 < j < N - 1)$$

$$b_1^N = E_x^N \frac{h^N}{2}, \quad b_2^N = G_{xz}^N \quad (j = N)$$

$$d_1^{11} = E_x^1 \frac{h^1}{3}, \quad d_2^{11} = \frac{G_{xz}^1}{h^1} \quad (j = 1)$$

$$d_1^{jj} = E_x^{j-1} \frac{h^{j-1}}{3} + E_x^j \frac{h^j}{3}, \quad d_2^{jj} = \frac{G_{xz}^{j-1}}{h^{j-1}} + \frac{G_{xz}^j}{h^j} \quad (2 < j < N - 1)$$

$$d_1^{NN} = E_x^N \frac{h^N}{3}, \quad d_2^{NN} = \frac{G_{xz}^N}{h^N} \quad (j = N)$$

For $i \neq j$:

$$d_1^{ij} = E_x^j \frac{h^j}{6}, \quad d_2^{ij} = -\frac{G_{xz}^j}{h^j} \quad (j = i \pm 1)$$

$$d_1^{ij} = d_2^{ij} = 0 \quad (j \neq i \pm 1)$$

When failure is detected at a Gauss point by a given failure criterion, stiffness properties are adjusted by degradation factors according to the failure mode (see Section 3), and subsequently the equivalent moduli in Equation (3), E_x and G_{xz} , are modified. Using these modified equivalent moduli, which are computed at

the top and bottom of each layer, the stiffness coefficients are expressed as follows:

$$a_1 = \sum_{k=1}^N \frac{1}{2} [E_x^{k(top)} + E_x^{k(bottom)}] h^k, \quad a_2 = \sum_{k=1}^N \frac{1}{2} [G_{xz}^{k(top)} + G_{xz}^{k(bottom)}] h^k$$

For $i = j$:

$$b_1^1 = \left[\frac{1}{4} E_x^{1(top)} + \frac{3}{4} E_x^{1(bottom)} \right] \frac{h^1}{2}, \quad b_2^1 = -\frac{1}{2} [G_{xz}^{1(top)} + G_{xz}^{1(bottom)}]$$

$$(j = 1)$$

$$b_1^j = \left[\frac{1}{4} E_x^{j-1(top)} + \frac{3}{4} E_x^{j-1(bottom)} \right] \frac{h^{j-1}}{2} + \left[\frac{3}{4} E_x^{j(top)} + \frac{1}{4} E_x^{j(bottom)} \right] \frac{h^j}{2}$$

$$b_2^j = \frac{1}{2} [G_{xz}^{j-1(top)} + G_{xz}^{j-1(bottom)}] - \frac{1}{2} [G_{xz}^{j(top)} + G_{xz}^{j(bottom)}]$$

$$(2 < j < N - 1)$$

$$b_1^N = \left[\frac{3}{4} E_x^{N(top)} + \frac{1}{4} E_x^{N(bottom)} \right] \frac{h^N}{2}, \quad b_2^N = -\frac{1}{2} [G_{xz}^{N(top)} + G_{xz}^{N(bottom)}]$$

$$(j = N)$$

$$d_1^{11} = [E_x^{1(top)} + 7E_x^{1(bottom)}] \frac{h^1}{24}, \quad d_2^{11} = [G_{xz}^{1(top)} + G_{xz}^{1(bottom)}] \frac{1}{2h^1}$$

$$(j = 1)$$

$$d_1^{jj} = [7E_x^{j-1(top)} + E_x^{j-1(bottom)}] \frac{h^{j-1}}{24} + [E_x^{j(top)} + 7E_x^{j(bottom)}] \frac{h^j}{24}$$

$$d_2^{jj} = [G_{xz}^{j-1(top)} + G_{xz}^{j-1(bottom)}] \frac{1}{2h^{j-1}} + [G_{xz}^{j(top)} + G_{xz}^{j(bottom)}] \frac{1}{2h^j}$$

$$(2 < j < N - 1)$$

$$d_1^{NN} = [7E_x^{N(top)} + E_x^{N(bottom)}] \frac{h^N}{24}, \quad d_2^{NN} = [G_{xz}^{N(top)} + G_{xz}^{N(bottom)}] \frac{1}{2h^N}$$

$$(j = N)$$

For $i \neq j$:

$$d_1^{ij} = \frac{1}{2} [E_x^{j(top)} + E_x^{j(bottom)}] \frac{h^j}{6}, \quad d_2^{ij} = -\frac{1}{2} [G_{xz}^{j(top)} + G_{xz}^{j(bottom)}] \frac{1}{h^j}$$

$$(j = i \pm 1)$$

$$d_1^{ij} = d_2^{ij} = 0 \quad (j \neq i \pm 1)$$

REFERENCES

1. Vinson, J. R. and R. L. Sierakowski. 1987. *The Behavior of Structures Composed of Composite Materials*. Dordrecht, Martinus Nijhoff Publishers.
2. Lee, J. D. 1982. "Three Dimensional Finite Element Analysis of Damage Accumulation in Composite Laminate," *Computers & Structures*, 15(3):335-350.
3. Ochoa, O. O. and J. J. Engblom. 1987. "Analysis of Progressive Failure in Composites," *Composite Science and Technology*, 28:87-102.
4. Leichti, R. J. and R. C. Tang. 1989. "Predicting the Load Capacity of Wood Composite I-Beams Using the Tensor Polynomial Strength Theory," *Wood Science and Technology*, 23:109-121.
5. Hwang, W. C. and C. T. Sun. 1989. "Failure Analysis of Laminated Composites by Using Iterative Three-Dimensional Finite Element Method," *Computers & Structures*, 33(1):41-47.
6. Tolson, S. and N. Zabaras. 1991. "Finite Element Analysis of Progressive Failure in Laminated Composite Plates," *Computers & Structures*, 38(3):361-376.
7. Tan, S. C. 1991. "A Progressive Failure Model for Composite Laminates Containing Openings," *J. Composite Materials*, 25:556-577.
8. Tan, S. C. and J. Perez. 1993. "Progressive Failure of Laminated Composite with a Hole under Compressive Loading," *J. Reinforced Plastics and Composites*, 12:1043-1057.
9. Reddy, Y. S. and J. N. Reddy. 1993. "Three-Dimensional Finite Element Progressive Failure Analysis of Composite Laminates under Axial Tension," *J. Composites Technology & Research*, 15(2):73-87.
10. Greif, R. and E. Chapon. 1993. "Investigation of Successive Failure Modes in Graphite/Epoxy Laminated Composite Beams," *J. Reinforced Plastics and Composites*, 12(5):602-621.
11. Davalos, J. F., H. A. Salim and U. Munipalle. 1992. "Glulam-GFRP Composite Beams for Stress-Laminated T-System Timber Bridges," *1st International Conference on Advanced Composite Materials in Bridges and Structures*, CSCE-CGC, Sherbrooke (Quebec), Canada, pp. 455-463.
12. Kim, Y., J. F. Davalos and E. J. Barbero. 1994. "Composite Beam Element with Layerwise Plane Sections," *J. Engineering Mechanics*, ASCE, 120(5):1160-1166.
13. Davalos, J. F., Y. Kim and E. J. Barbero. 1994. "Analysis of Laminated Beams with a Layer-Wise Constant Shear Theory," *Composite Structures*, 28:241-253.
14. Lopez-Anido, R., J. F. Davalos and E. J. Barbero. 1995. "Experimental Evaluation of Stiffness of Laminated Composite Beam Elements under Flexure," *J. Reinforced Plastics and Composites*, 14:349-361.
15. Groves, S. E., C. E. Harris, A. L. Highsmith and R. G. Norvell. 1987. "An Experimental and Analytical Treatment of Matrix Cracking in Cross-Ply Laminates," *Experimental Mechanics*, 27(1):73-79.
16. Kim, Y. 1995. "A Layer-Wise Theory for Linear and Failure Analysis of Laminated Composite Beams," Ph.D. dissertation, College of Engineering, West Virginia University, Morgantown, WV.

Mi
F

ABSTRACT
Ti-6Al-4V
pyrolytic c
ering both
tropic. Th
most other
nificant eff
ties and im
posed. Th
and comp
erties of S

KEY WORDS
modelling

SILICO
S consi
with thei
duced re
fibre and

*Research
**Professor

Journal